Applied Catalysis B: Environmental 188 (2016) 134–146

Contents lists available at ScienceDirect

Applied Catalysis B: Environmental

journal homepage: www.elsevier.com/locate/apcatb

Photocatalytic removal of patent blue V dye on Au-TiO_2 and Pt-TiO_2 catalysts

Vincenzo Vaiano[a,*], Giuseppina Iervolino[a], Diana Sannino[a], Julie J. Murcia[b], Maria C. Hidalgo[c], Paolo Ciambelli[a], José A. Navío[c]

[a] Department of Industrial Engineering, University of Salerno, via Giovanni Paolo II, 132, 84084 Fisciano, SA, Italy
[b] Grupo de Catálisis de la Universidad Pedagógica y Tecnológica de Colombia, Avenida Central del Norte, Tunja, Boyacá, Colombia
[c] Instituto de Ciencia de Materiales de Sevilla (ICMS), Consejo Superior de Investigaciones Científicas (CSIC), Universidad de Sevilla, Américo Vespucio 49, 41092 Sevilla, Spain

ARTICLE INFO

Article history:
Received 26 October 2015
Received in revised form 26 January 2016
Accepted 1 February 2016
Available online 3 February 2016

Keywords:
Photocatalysis
Patent blue V dye
Au-TiO_2
Pt-TiO_2
Photocatalysts preparation method

ABSTRACT

In this work it was studied the efficiency of a photocatalytic process for the removal of patent blue V. This dye is very difficult to remove by conventional treatments such as adsorption or coagulation therefore the photocatalytic process is a very interesting alternative for the removal this dye mainly because it does not require expensive oxidants and it can be carried out at mild temperatures and pressures. In this work it was tested the efficiency of Au-TiO_2 and Pt-TiO_2 photocatalysts in the Patent blue V removal. The Au-TiO_2 catalysts were prepared by two different methods: chemical reduction and photochemical deposition; Pt-TiO_2 catalysts were obtained only by photochemical deposition. In the synthesis of the catalysts prepared by photochemical deposition, it was evaluated the influence of some parameters, such as deposition time and the intensity of the light source over the physicochemical properties and photocatalytic activity of the materials obtained. An analysis of the effect of the catalyst dosage and initial patent blue V concentration over the dye degradation efficiency was also attempted.

In general, it was observed that the presence of Au or Pt on TiO_2 enhances the patent blue V photodegradation; it was found that noble metal particle size and distribution on TiO_2 surface are important factors influencing the dye removal. The highest dye degradation was obtained over the Au-TiO_2 catalyst prepared by photochemical deposition, using high light intensity and 15 min of deposition time during the synthesis. A discoloration and a total organic carbon (TOC) removal of 93 and 67% respectively, were obtained over this material after 180 min of UV irradiation. These values are higher than that the obtained on S-TiO_2 (discoloration and TOC removal of about 25% and 3%, respectively).

1. Introduction

A substantial amount of hazardous organic compounds are introduced into the environment as a result of the industrial activities. Currently, dyestuffs coming from textile and food industries are important pollutants in water effluents. These dyes represent a serious problem for the human and animal health. For that reason, the degradation of these pollutants has acquired increasing attention. Heterogeneous photocatalysis has been studied in the decomposition of a wide range of undesirable chemical contaminants and it appears to be a feasible process for the degradation of dyes in water courses by using solar or artificial light illumination [1–4]. TiO_2 is the semiconductor most widely studied and used in photocatalytic processes. In order to improve the photoactivity of this oxide, many strategies, such as sulfation and noble metal addition, have been employed [3,5,6]. For the noble metal addition on TiO_2 surface, many methods have been employed, resulting in different metal particle sizes. The presence of metal nanoparticles decreases the electron-hole recombination, thus improving the TiO_2 efficiency in the photodegradation reactions. It has been reported that the improvement of TiO_2 photoactivity by noble metal addition depends not only on metal content but also on TiO_2 properties, metal particle size and metal oxidation state [7–10]. So it is very important to control the synthesis parameters in order to obtain highly effective photocatalysts based on modified TiO_2.

Patent blue V (PB) is a recognized dye in food industry. This compound is difficult to remove with conventional treatments such as adsorption or coagulation. As alternative the photocatalytic degradation of PB has been investigated and reported in literature by using TiO_2 in presence of different electron acceptors such as H_2O_2

* Corresponding author.
E-mail address: vvaiano@unisa.it (V. Vaiano).

http://dx.doi.org/10.1016/j.apcatb.2016.02.001
0926-3373/

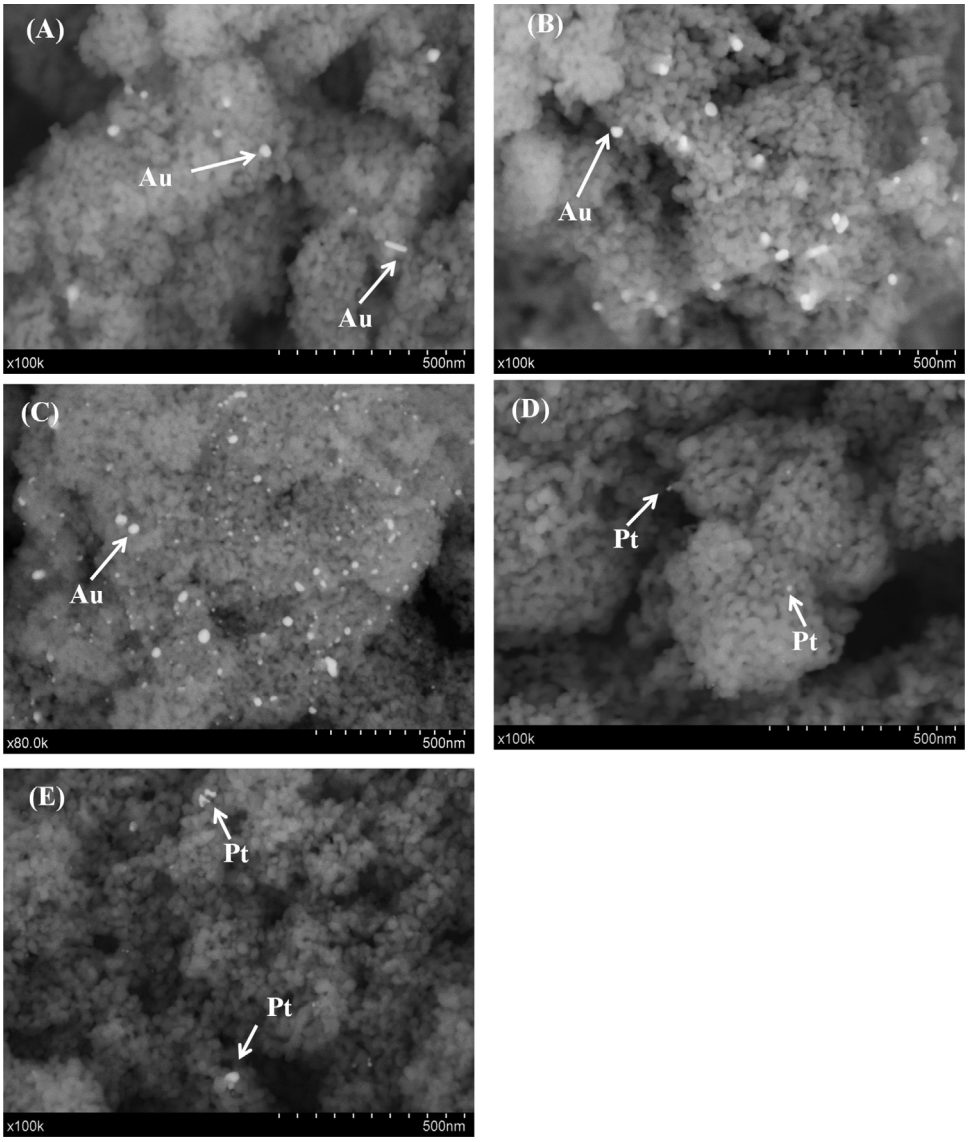

Fig. 1. SEM images of photocatalysts synthesized using different methods: photodeposition (PD) and chemical reduction (CR). (A) Au-TiO_2(PD-HI)15min; (B) Au-TiO_2(PD-HI)120min; (C) Au-TiO_2(CR); (D) Pt-TiO_2(PD-HI)15min and (E) Pt-TiO_2(PD-HI)120min.

or $KBrO_3$ [11,12] or using TiO_2-coated nonwoven fibers [13]. In the present work it was evaluated the photodegradation of the PB over sulfated and metallized TiO_2 (Au-TiO_2 and Pt-TiO_2). It was also evaluated the effect of the Au or Pt addition and the synthesis parameters over the efficiency of these materials in the PB removal. At our knowledge, it is the first paper reporting the use of TiO_2 metallized with noble metals in a photocatalytic system for the removal of PB dye.

2. Experimental

2.1. Synthesis of the photocatalysts

2.1.1. Sulfated TiO_2

TiO_2 used as starting material was prepared by the hydrolysis of titanium tetraisopropoxide (Aldrich, 97%) in isopropanol solution (1.6 M) by the slow addition of distilled water (volume ratio isopropanol/water 1:1). Afterward, the generated precipitate was filtered, dried at 110 °C overnight and calcined at 650 °C for 2 h. Sulfation treatment was applied to TiO_2 before calcination; the TiO_2 powders were sulfated by immersion in H_2SO_4 aqueous solution 1 M for 1 h and afterward calcinated at 650 °C for 2 h (S-TiO_2). Sulfation treatment was carried out for two reasons; on one hand, previous results have shown that sulfation stabilizes the anatase phase up to high temperatures and protect the catalyst from the loss of surface area by sintering [14]. On the other hand, at the calcination temperature of 650 °C, the elimination of sulfate groups promotes the creation of high number of oxygen vacancies, which have been reported as preferential sites for noble metal adsorption [15].

The S-TiO_2 powders were also modified by noble metal addition. Two different methods were employed: the photochemical deposition and chemical reduction method. The typical procedure is described as follows.

2.1.2. Photochemical deposition (PD) of gold and platinum over S-TiO_2

Gold (III) chloride trihydrate ($HAuCl_4{\cdot}3H_2O$, Aldrich 99.9%) or hexachloroplatinic acid (H_2PtCl_6, Aldrich 99.9%) were used as metal precursors for Au and Pt, respectively. Under an inert

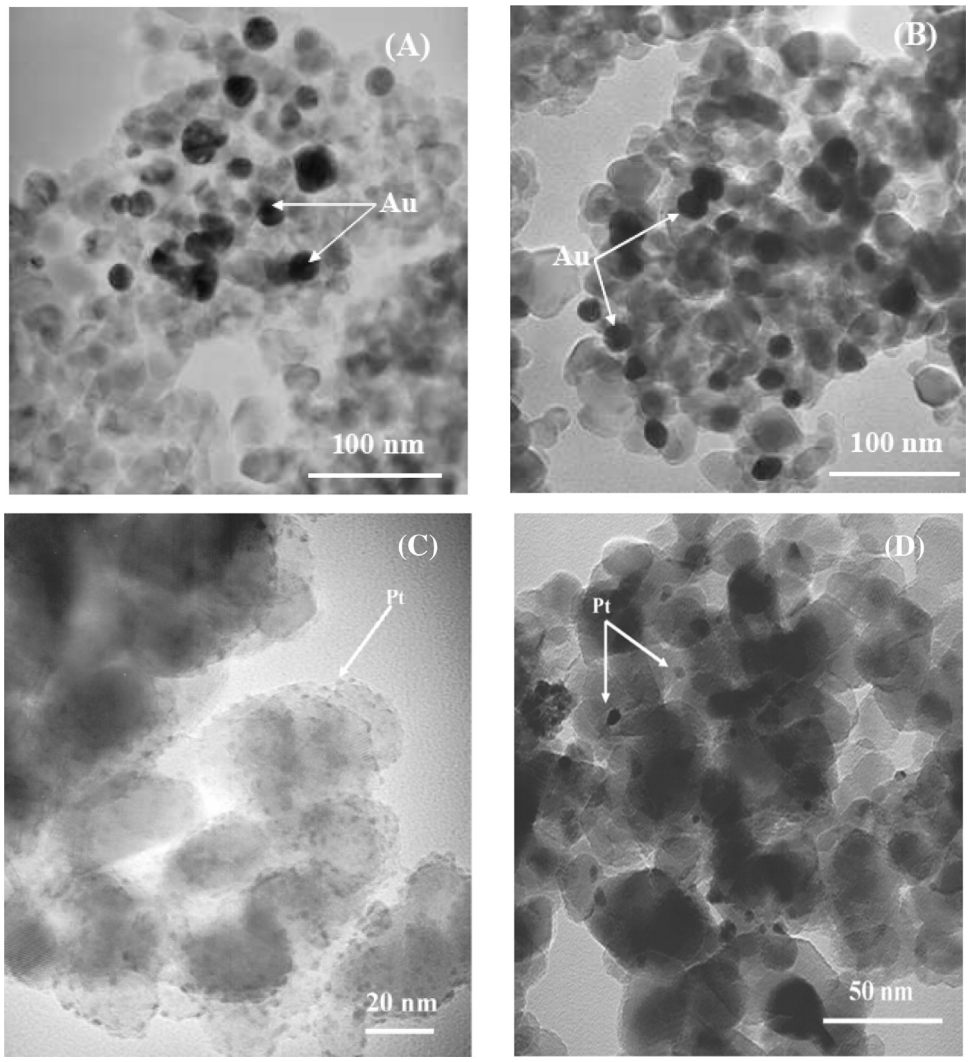

Fig. 2. TEM images of metallized S-TiO_2. (A) and (B) Au-TiO_2 catalysts prepared by PD method using 140 W/m^2 of light intensity and different deposition time 15 and 120 min, respectively. (C) and (D) Pt-TiO_2 samples prepared by photodeposition method and different deposition time 15 and 120 min, respectively.

atmosphere (N_2), a suspension of S-TiO_2 in distilled water containing isopropanol (Merck 99.8%) which acts as sacrificial donor, was prepared. Then, the appropriate amount of metal precursor to obtain a nominal Pt or Au loading of 0.5 weight total (wt%) to TiO_2 was added. Final pH of the suspensions was 3. Photochemical deposition of Pt or Au was then performed by illuminating the suspensions with an Osram Ultra-Vitalux lamp (300W) with a sun-like radiation spectrum and a main emission line in the UVA range at 365 nm, using 15 and 120 min of photodeposition time. Light intensities on the TiO_2 surface were low intensity 0.15 W/m^2 (LI) and high intensity 140 W/m^2 (HI) for Pt and Au photochemical deposition, respectively.

After noble metal deposition, the powders were recovered by filtration and dried at 110 °C overnight. The metallized samples were called Au-TiO_2 and Pt-TiO_2.

2.1.3. Chemical reduction (CR) of gold over S-TiO_2

Chemical reduction of gold was carried out by using sodium citrate as both reducing and stabilizing agent following a procedure described in the literature [16]. Appropriate amount of $HAuCl_4$ for nominal content of deposited Au of 0.5 wt.% with respect to TiO_2 was dissolved in distilled water (1 mg $HAuCl_4$/10 mL water). Then, suspensions of the different TiO_2 samples (1 g) in sodium citrate solutions (0.2 g/10 mL distilled water) were added. The final suspensions were heated to reflux for 1 h under N_2 atmosphere to avoid gold re-oxidation. After this time, the powders were washed, filtered and dried at 110 °C overnight.

All the photocatalysts synthesized are enlisted in Table 1.

2.2. Characterization of the photocatalysts

All the materials were widely characterized using different techniques. Specific surface area (S_{BET}) measurements were carried out using low-temperature N_2 adsorption in a Micromeritics ASAP 2010 instrument. Degasification of the samples was performed at 150 °C.

Gold and platinum particles morphology was evaluated by Scanning electron microscopy (SEM), Field Emission SEM images were obtained in a Hitachi S-4800 microscope. Transmission Electron Microscopy (TEM) was performed in a Philips CM200 instrument. In both techniques, samples were dispersed in ethanol using an ultrasonicator and dropped on a carbon grid.

Determination of the metal particle average diameter ($\bar{d}$) in the different samples was accomplished by counting particles in a high number of TEM images from different places of the samples. The following equation was used: ($\bar{d}$ nm) = $\Sigma di\ x\ fi$

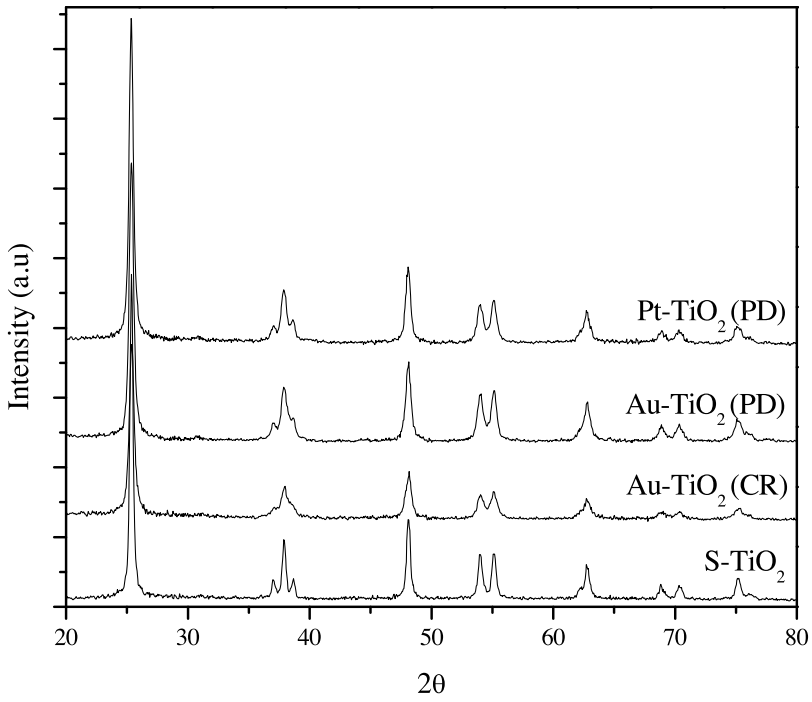

Fig. 3. XRD patterns for TiO_2 and M-TiO_2 photocatalysts (M = Au or Pt) prepared by chemical reduction (CR) and photochemical deposition (PD) using 120 min of deposition time.

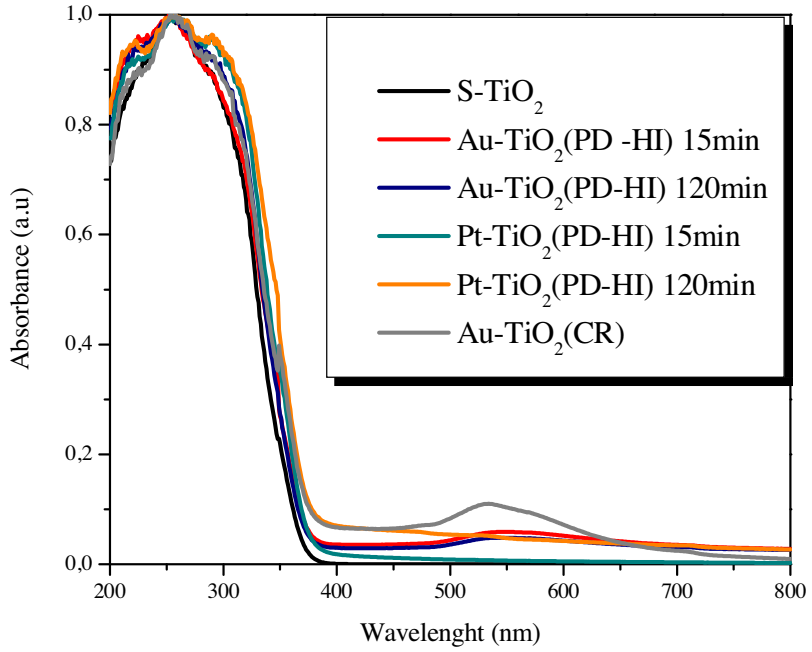

Fig. 4. UV–vis DRS spectra for the investigated photocatalysts.

Where *di* is the diameter of the *ni* counted particles and *fi* is the particle size distribution estimated by:

$$fi = \frac{ni}{\sum ni}$$

where *ni* is the number of particles of diameter *di*.

Crystalline phase composition and degree of crystallinity of the samples were estimated by X-ray diffraction (XRD). XRD patterns were obtained on a Siemens D-501 diffractometer with Ni filter and graphite monochromator using Cu Kα radiation. Anatase crystallite sizes were calculated from the line broadening of the main anatase X-ray diffraction peak (1 0 1) by using the Scherrer equation. Peaks were fitted by using a Voigt function.

Light absorption properties of the samples were studied by UV–vis spectrophotometry. The UV–vis DR spectra were recorded on a Varian spectrophotometer model Cary 100 equipped with an integrating sphere and using $BaSO_4$ as reference. Band-gaps values were calculated from the corresponding Kubelka–Munk functions, $F(R\infty)$, which are proportional to the absorption of radiation by

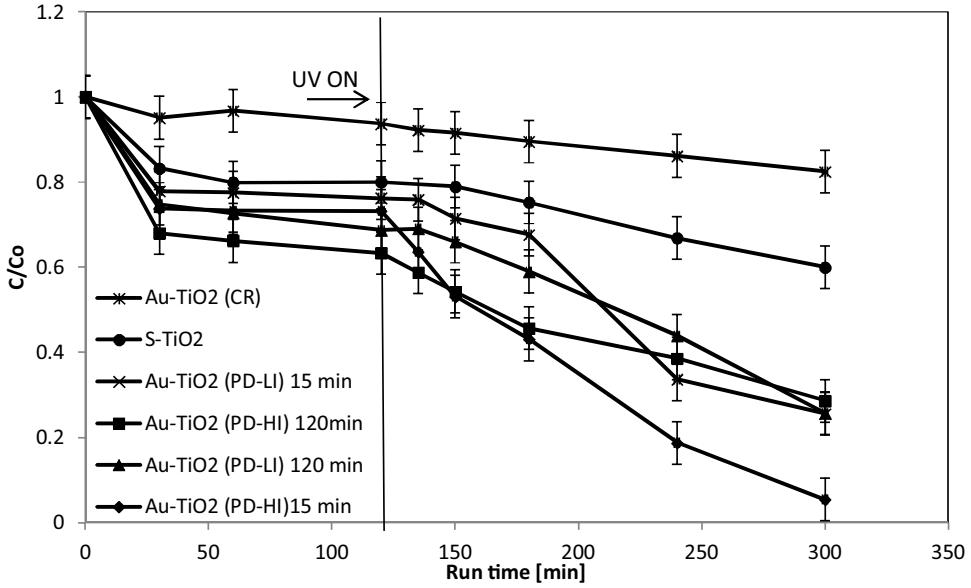

Fig. 5. Discoloration of the Patent blue V as a function of run time over the photocatalysts analyzed; Patent blue V initial concentration: 7 mg/L; catalyst dosage: 3 g/L.

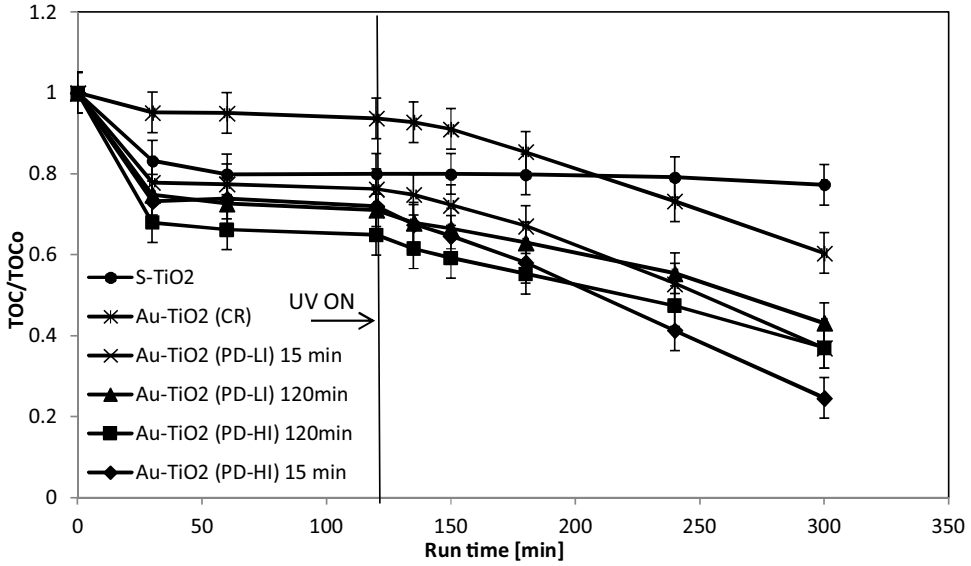

Fig. 6. Total Organic Carbon (TOC) removal as a function of run time over the catalysts analyzed. Patent Blue V initial concentration: 7 mg/L; catalyst dosage: 3 g/L.

Table 1
Summary of the characterization results.

Catalyst	Method for metal addition	Light intensity (W/m^2)	Deposition time (min)	S_{BET} (m^2/g)	Average metal particle size (nm)	$D_{Anatase}$ (nm)	Band gap (eV)	wt.% metal content (XRF)	Binding energy (eV)	
									Ti $2p_{3/2}$	O 1s
S-TiO_2	–	–	–	58	–	20	3.20	–	458.5	529.8
Au-TiO_2	Chemical reduction (CR)	–	–	52	7–8	20	3.22	0.39	458.3	529.7
	Photochemical Deposition (PD)	0.15 (LI)[a]	15	57	8–10	20	3.19	0.29	459.0	530.3
			120	58	11–12	19	3.24	0.32	458.5	529.8
		140 (HI)[a]	15	54	30–40	21	3.20	0.36	459.6	530.8
			120	53	40–50	20	3.21	0.45	458.8	530.1
Pt-TiO_2		140 (HI)[a]	15	53	2–3	23	2.80	0.26	458.5	529.9
			120	59	4–6	21	2.80	0.41	458.4	529.6

[a] (LI) = Low intensity and (HI) = High intensity.

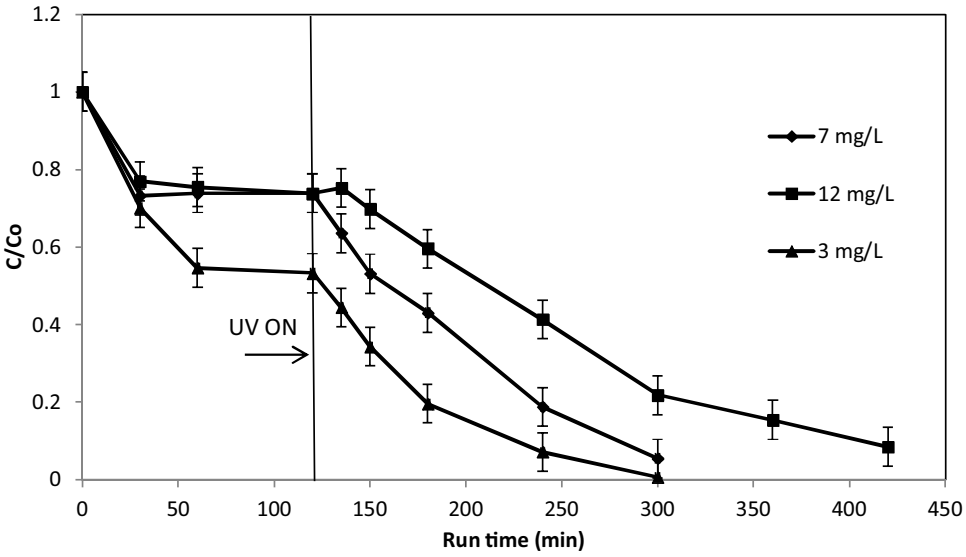

Fig. 7. Patent blue V discoloration over Au-TiO_2(PD-HI) 15min catayst, varying the initial concentration of the dye; catalyst dosage: 3 g/L.

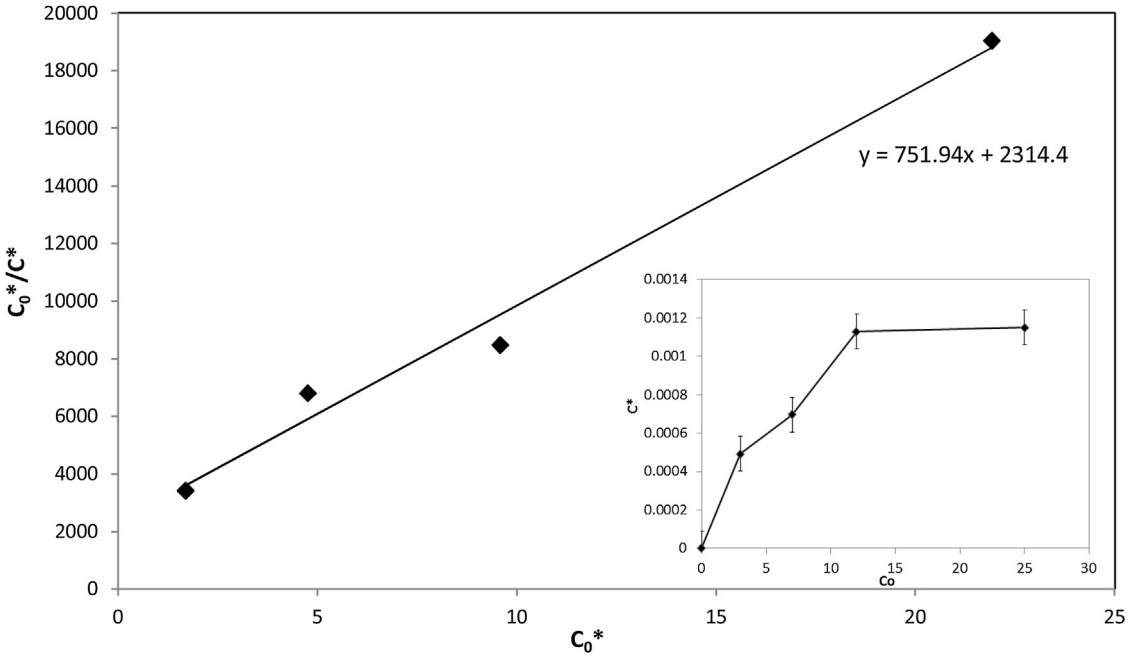

Fig. 8. Evaluation of Patent blue V adsorption constant on Au-TiO_2(PD-HI) 15 min catalyst; catalyst dosage: 3 g/L.

plotting $(F(R\infty) \times h\upsilon)^{1/2}$ against $h\upsilon$ [6]. Chemical composition and total noble metals content in the samples were determined by X-ray fluorescence spectrometry (XRF) in a Panalytical Axios sequential spectrophotometer equipped with a rhodium tube as the source of radiation. XRF measurements were performed onto pressed pellets (sample included in 10 wt% of wax).

X-ray photoelectron spectroscopy (XPS) studies were carried out on a Leybold–Heraeus LHS-10 spectrometer, working with constant pass energy of 50 eV. The spectrometer main chamber, working at a pressure $<2 \times 10^{-9}$ Torr, is equipped with an EA-200MCD hemispherical electron analyzer with a dual X-ray source working with Al Kα ($h\upsilon = 1486.6$ eV) at 120 W and 30 mA. C 1s signal (284.6 eV) was used as internal energy reference in all the experiments. Samples were outgassed in the prechamber of the instrument at 150 °C up to a pressure $<2 \times 10^{-8}$ Torr to remove chemisorbed water.

2.3. Photocatalytic experiments

Photocatalytic experiments were carried out with a Pyrex cylindrical reactor (ID = 2.5 cm) equipped with an air distributor device. The photoreactor was irradiated by a strip composed of 15 UV-LEDs (nominal power: 10W) with wavelength emission in the range 375–380 nm. The LEDs strip was positioned around the external surface of the reactor so that the light source uniformly irradiated the reaction volume (light intensity: 570 W/m^2). The catalyst dosage was 3 g/L in an 80 mL aqueous solution containing 7 mg/L of PB. Continuous mixing of the solution in the reactor was assured by external recirculation of water through a peristaltic pump; the suspension was left in dark conditions for 120 min to reach the adsorption-desorption equilibrium of PB on the photocatalysts surface, and then the photocatalytic reaction was initiated under UV light for up to 180 min.

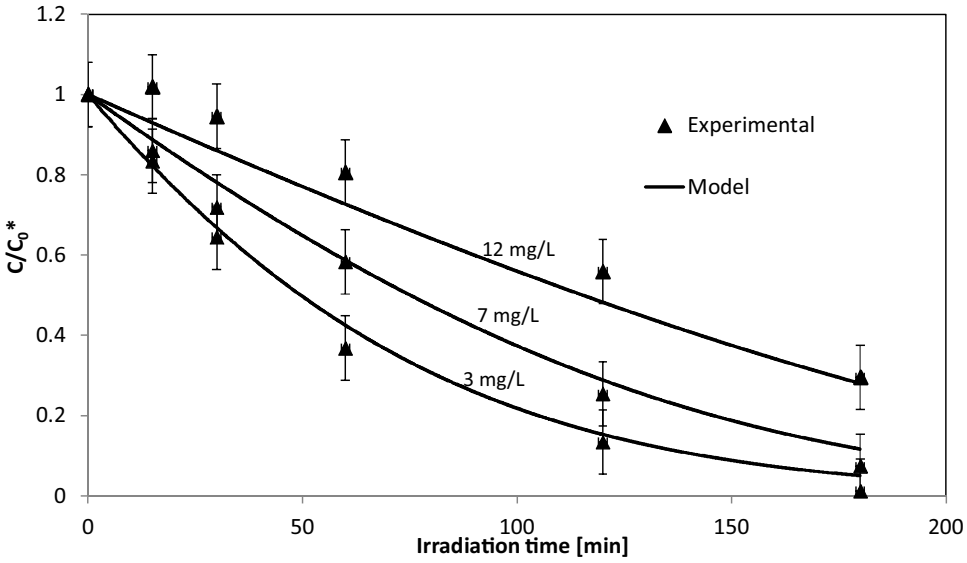

Fig. 9. Experimental and predicted data as a function of Patent blue V initial concentration on Au-TiO_2(PD-HI) 15min; catalyst dosage: 3 g/L.

In order to compare the effect of the dye concentration and the photocatalyst dosage, different values of these parameters were evaluated. Thus, the initial concentrations of patent blue were 3, 7 and 12 mg/L; the catalysts dosages were 3, 6, 9 and 12 g/L.

2.4. Analytical measurements

The color of aqueous samples was determined with a Perkin Elmer UV–vis spectrophotometer at λ_{max} = 635 nm. The TOC was measured by the high temperature combustion method on a catalyst (Pt-Al_2O_3) in a tubular flow microreactor operated at 680 °C, with a stream of hydrocarbon free air to oxidize the organic carbon. Laboratory apparatus consisted of mass flow controllers (Brooks) operating on each gas; an injection system; a NDIR continuous analyzer (Hartmann & Braun Uras 10E) for measurements of CO and CO_2 concentrations at the combustion reactor outlet and a paramagnetic analyzer (Hartmann & Braun Magnos 6G) for continuous monitoring of O_2.

3. Results and discussion

3.1. Characterization of the photocatalysts

In order to correlate the physicochemical properties of the catalysts with their photocatalytic activity, all the materials were widely characterized by using different techniques and the results obtained are summarized in Table 1 and presented below.

3.1.1. N_2 physisorption

The specific surface areas (S_{BET}) of the photocatalysts analyzed are listed in Table 1. As it can be observed, the BET surface area of S-TiO_2 is 58 m^2/g. After the metal addition a slight decrease of the S_{BET} value was detected, probably due to pore blocking by metal nanoparticles homogeneously distributed on surface. As it can be seen in Table 1, this effect is much more noticeable in the catalysts prepared by chemical reduction and also in the materials prepared by photochemical deposition method using 15 min of deposition time.

3.1.2. Microscopic analysis

In order to obtain information about the metal deposits size and dispersion, all the samples modified by gold or platinum addition were studied by SEM. Fig. 1 shows representative SEM images of the metallized samples prepared by chemical reduction (CR) and photochemical deposition method (PD), using 140 W/m^2 of light intensity (HI) and different deposition times (15 and 120 min). Images of the samples prepared using low intensity (LI = 0.15 W/m^2) are not provided for the sake of brevity. In all the samples, gold or platinum particles can be seen as white spots placed over the larger TiO_2 particles. As it can be observed, there are significant differences in particles sizes and morphology between samples prepared by PD or by CR. Thus, in the catalyst Au-TiO_2 prepared by CR (Fig. 1C), the gold particles are more homogeneously distributed on TiO_2 surface than the gold particles observed in the samples prepared by PD (Fig. 1A and B). The higher number of gold particles covering the TiO_2 surface can explain the lowest S_{BET} value observed in the sample prepared by CR (Table 1).

It was also possible to observe that the platinum particles are smaller than the gold particles in the metallized samples prepared by PD, and in all the cases the number and size of the metal particles increase with the deposition time from 15 to 120 min. The average particle size of the noble metal (Au or Pt) particles, obtained by TEM analysis is presented in Table 1; selected TEM images of the samples metallized prepared by photochemical deposition method, using the highest light intensity and different deposition times are presented in Fig. 2. In these images it is possible to observe that gold particles with higher sizes are heterogeneously distributed and partially covering the TiO_2 surface; the number and the size of the gold particles increases with the deposition time. On the contrary, in the case of the Pt-TiO_2 sample, platinum particles with the lowest sizes are homogeneously covering the titania surface.

3.1.3. X-ray diffraction (XRD)

XRD was used to analyze the effect of the metal addition on the crystallite structure and phase composition of sulfated TiO_2. Fig. 3 shows the XRD patterns of the sulfated TiO_2 and the metallized catalysts prepared by CR and PD using high light intensity and 120 min of deposition time.

In all the analyzed samples, only anatase peaks (25.3°, 38.0°, 48.0° and 54.7° 2θ) were detected. The stabilization of anatase phase of the TiO_2 by the sulfation pretreatment can be noticed here, as no traces of rutile were found even after the high calcination temperature used during the preparation of the catalysts [14].

The anatase crystallite size in the different samples was determined from the broadening of corresponding X-ray diffraction peaks by using Scherrer equation and these data are listed in Table 1. As it can be observed, for sulfated samples the anatase crystallite size was about 20 nm, any important influence of the synthesis parameters over this value was observed. No peaks ascribed to platinum or gold species were detected in the XRD patterns of the metallized samples; surely due to the low metal content in the samples or due to the detection limit of this technique.

XRD patterns of the catalysts prepared by PD under low light intensity are not included for the sake of brevity, but the diffraction peaks are similar than the observed for the samples obtained at high light intensity.

3.1.4. UV–vis diffuse reflectance spectra (UV–vis DR)

The UV–vis DR spectra of selected samples are shown in Fig. 4. The typical band edge of the TiO_2 semiconductor was observed at around of 370 nm for all the samples. Gold or platinum addition did not alter substantially the absorption properties of the samples; however, a slight increase of absorbance throughout the visible range of the spectrum was observed due to the purple or grey color of the metallized materials, respectively. In the Au-TiO_2 catalysts, the surface plasmon resonance band of metallic gold can be observed; this characteristic plasmon is located around 550 nm. It is known that for colloidal gold nanoparticles there is a strong dependence between particle size and plasmon bandwidth and position [17–19].

From the UV–vis DR spectra, band gaps energies were calculated and the obtained results are reported in Table 1, being 3.20 eV for the S-TiO_2 sample. Any important modification of this value was observed after gold addition. A slight decrease of the band gap value was observed in the Pt-TiO_2 samples.

3.1.5. X-ray fluorescence

The real gold and platinum content in the metallized samples was measured by XRF and the results are enlisted in Table 1. As it can be seen, these values are under the nominal metal content used to prepare these materials (0.5 wt.%), thus indicating an incomplete reduction of the metal precursor on TiO_2 surface during the synthesis process. However, it was observed that the amount of deposited gold or platinum increases with the deposition time and with the light intensity in the materials prepared by PD method.

XRF analysis revealed that a certain amount of S and Cl^- species remained on the solids after preparation. The sulfur content in the samples was under 0.16 wt%; the Cl^- content in all the platinized samples was under 0.10 wt%; this content comes from the gold and platinum precursors.

3.1.6. X-ray photoelectron spectroscopy (XPS)

XPS analyzes were also carried out and the binding energies (BE) of the main XPS peaks (Ti $2p_{3/2}$ and O 1s) for the different samples are enlisted in Table 1. The Ti $2p_{3/2}$ core level spectra were similar for all the analyzed samples with peaks centered at 458.4 ± 0.1 eV, corresponding to Ti^{4+} in the TiO_2 network as the main component. In the O 1s region, a peak located at a binding energy of 529.8 ± 0.2 eV was registered in all the samples. This peak is assigned to lattice oxygen in TiO_2, with a broad shoulder at higher binding energies ascribed to oxygen in surface hydroxyl groups.

From the XPS data, O/Ti ratios were also calculated and it was found that for S-TiO_2 sample the O/Ti value was 1.70 indicating the presence of a certain amount oxygen vacancies on the surface of this oxide, in agreement with previous reported results [14] that showed the development of oxygen vacancies on TiO_2 surfaces due to the sulfation process. The ratios O/Ti for the metallized samples were higher than the observed in the S-TiO_2 sample, suggesting that the oxygen vacancies are partially annihilated during the Pt or Au photochemical deposition over the sulfated oxide. The atomic percentage of metal was calculated by XPS and it was found to be <0.2% in all the catalysts; in correlation with the XRF results, the metal atomic content increases with the deposition time and also with the light intensity used in the catalysts preparation.

Table 2
Percentage of discoloration and mineralization of the Patent blue V; initial dye concentration: 7 mg/L; catalyst dosage: 3 g/L.

Catalyst	Discoloration (%)	Mineralization (%)
S-TiO_2	25	3
Au-TiO_2(CR)	12%	35%
Au-TiO_2(PD-LI) 15min	67%	51%
Au-TiO_2(PD-LI) 120min	63%	37%
Au-TiO_2(PD-HI) 15min	93%	66%
Au-TiO_2(PD-HI) 120min	55%	29%
Pt-TiO_2(PD-HI) 15min	74%	45%
Pt-TiO_2(PD-HI) 120min	85%	44%

3.2. Photocatalytic activity results

3.2.1. Patent blue V photodegradation on Au-TiO_2

The efficiency of the photocatalysts prepared and characterized was evaluated in the PB removal. In order to verify that the target dye was converted in a heterogeneous photocatalytic process, blank experiments were performed. In particular, tests carried out in dark conditions did not evidence any oxidation activity. Moreover, additional control tests were carried out in the presence of PB dye and irradiating the photoreactor with UV-LEDs (photolysis reaction) and in the absence of photocatalyst. Also in this case, no degradation of the target dye was detected.

Fig. 5 shows the evolution of the discoloration of the PB as a function of run time, obtained over Au-TiO_2 photocatalysts in comparison with S-TiO_2. In dark conditions a decrease of PB concentration was observed during the first 30 min of the test and it was almost unchanged up to 120 min, indicating that the adsorption equilibrium of dye on catalyst surface was reached. After the dark period, the solution was irradiated with UV light and the reaction started to occur. As it can be observed, an important decrease of the dye concentration was obtained in presence of Au on titania surface. The highest discoloration was observed on the catalyst Au-TiO_2 prepared by photochemical deposition method, using high light intensity (140 W/m^2) and 15 min of deposition time.

The evaluation of the TOC during the run time was also analyzed and the obtained results are represented in Fig. 6. In this case it was also observed that the highest mineralization of the dye was achieved on the sample Au-TiO_2(PD-HI) 15min. In particular, with this catalyst, a discoloration and a TOC removal (evaluated starting from the irradiation time) of 93 and 67% respectively, were obtained after 180 min of UV irradiation. These values are higher than that obtained on S-TiO_2 (discoloration and TOC removal of about 25% and 3%, respectively).

The percentage of discoloration and mineralization of the PB evaluated starting from the irradiation time is summarized in Table 2.

In the case of the Au-TiO_2 samples prepared with the highest deposition time (120 min), the decrease of the photocatalytic activity could be due to the big cluster of gold particles which can act as a recombination centers, thus reducing the effectiveness of these samples [20]. The best photocatalytic behavior was observed over the catalyst Au-TiO_2 prepared by photochemical deposition method, using high light intensity (140 W/m^2) and 15 min of deposition time. It could be due to a combined effect between two factors: (i) the presence of the gold nanoparticles, which act as a sink for the electrons, retarding the electron-hole recombination,

thus leading to an improvement of the TiO_2 photoefficiency; (ii) in this catalyst, the gold nanoparticles are heterogeneously distributed on TiO_2 surface. The lower number of the gold particles allows to the dye molecule to be adsorbed with the TiO_2 surface. In this case the azo or sulfate groups in the molecule of dye can act as electron donor [20], leading to a better interaction between substrate and catalyst surface, thus increasing the dye discoloration efficiency.

In the case of the catalysts with the lowest metal particle sizes, such as Au-TiO_2 prepared by chemical reduction or Pt-TiO_2 catalysts, many particles with low metal particle sizes could covering the TiO_2 surface, thus leading to difficult adsorption of the dye.

Finally, it is important to note that the lowest PB discoloration was obtained over the catalyst Au-TiO_2 prepared by CR. The discoloration obtained over this catalyst is even lower than the obtained with the starting S-TiO_2. This behavior could be related with the presence of remaining material on catalyst surface coming from the preparation procedure, mainly due to the sodium citrate used as reducing agent. Thus the remaining material on surface could have a detrimental effect over effectiveness of the Au-TiO_2(CR) catalyst on the dye photodegradation. These results can suggest that photodeposition is a suitable method to prepare active and efficient catalysts for PB photocatalytic removal.

3.2.2. *Patent blue V photodegradation on Au-TiO_2—effect of the initial dye concentration*

Taking into account that the best photocatalytic behavior in the PB removal was obtained on

Au-TiO_2(PD-HI) 15min catalyst, the effectiveness of this catalyst in the degradation of different initial concentrations (3, 7 and 12 mg/L) of the dye was evaluated.

Fig. 7, shows the dye discoloration on the Au-TiO_2(PD-HI) 15min catalyst. After 120 min of dark adsorption, the photocatalytic test started. After 180 min of irradiation, the final value of the discoloration was 100% in the case of 3 mg/L, 92% in the case of 7 mg/L and 20% in the case of 12 mg/L PB initial concentration.

For the interpretation of the effect of the dye initial concentration on the photodegradation performances, the Langmuir–Hinshelwood model has been used [21].

Considering that the adsorption equilibrium was reached after 120 min of run time, the behavior of the amount of PB adsorbed on catalyst as a function of the dye initial concentration (C_0) is similar to a Langmuir adsorption isotherm (Fig. 8 insert). Thus for the evaluation of PB adsorption on the active surface, the following equation was used:

$$C^* = \frac{b \times C_0^*}{1 + b \times C_0^*} \quad (1)$$

Where C* is the amount of PB adsorbed on catalyst (g_{dye}/g_{cat}); C_0^* is the concentration of PB in solution after dark adsorption (mg/L); b is the adsorption constant (L/mg).

The Langmuir isotherm can be rearranged to give:

$$\frac{C_0^*}{C^*} = \frac{1}{b \times C_m} + \frac{1}{C_m} C_0^* \quad (2)$$

Accordingly, a plot of C_0^*/C^* as a function of C_0^* produces a straight line with slope = $1/C_m$ and intercept = $1/bC_m$ (Fig. 8). C_m is the maximum absorbable value of C*.

The value of b was calculated from Eq. (2) utilizing the data reported in Fig. 8 and it was equal to 0.32 (L/mg).

With this value it was evaluated the apparent kinetic constant for all the initial concentration of dye, using the following equation:

$$\frac{dC(t)}{dt} = -K \times \frac{b \times C(t)}{1 + b \times C(t)} \times a \quad (3)$$

Where C(t) is the PB concentration (mg/L) as a function of irradiation time; *a* is the e catalyst dosage (g_{cat}/L) and K is the kinetic constant (mg/(g min)).

The initial condition of Eq. (3) is:

$t = 0$ $C(t) = C_0^*$

Eq. (3) together with the initial condition was solved with Euler iterative method to identify the constants K by fitting the experimental data as a function of irradiation time for the initial dye concentration of 7 mg/L. The fitting procedure was realized by using the least squares approach obtaining the value of K: 0.02 [mg/(g min)]. After obtaining the value of K, the experimental data obtained with different initial dye concentrations were fitted to analyze the ability of the model to predict the experimental data at 3 and 12 mg/L initial PB concentration. The obtained results are shown in Fig. 9.

The calculated values are in good agreement with all the experimental data. It is important to note that also for the higher initial

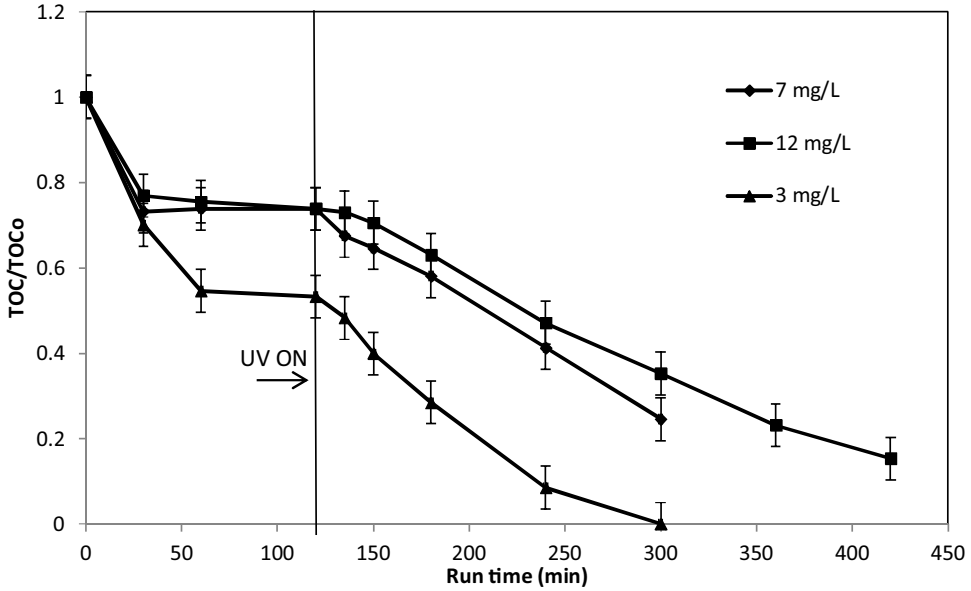

Fig. 10. Total Organic Carbon (TOC) removal over the Au-TiO_2(PD-HI) 15min catayst, varying the initial concentration of the dye; catalyst dosage: 3 g/L.

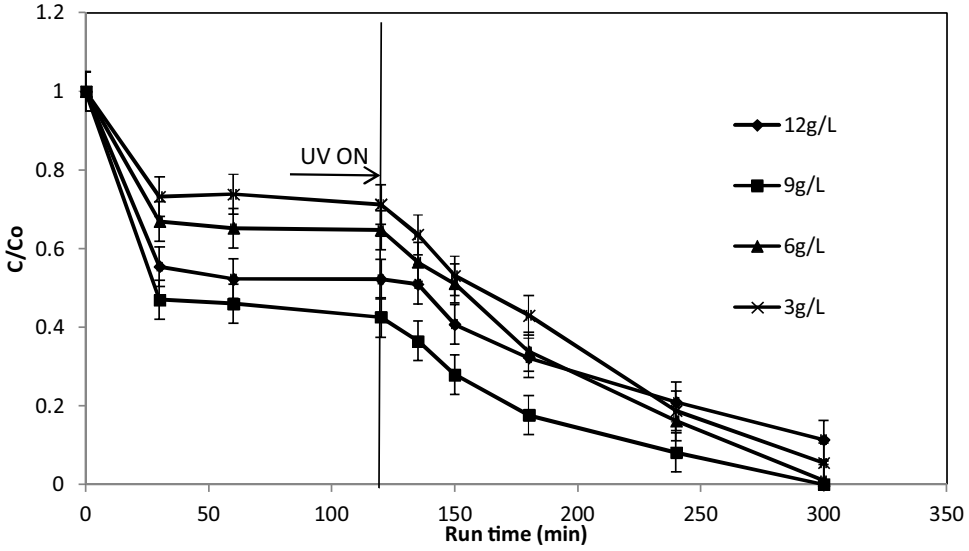

Fig. 11. Patent blue V discoloration over the Au-TiO_2(PD-HI) 15min catayst, varying the dosage of the photocatalyst (g/L); patent blue V initial concentration: 7 mg/L. (For interpretation of the references to colour in this figure legend, the reader is referred to the web version of this article.)

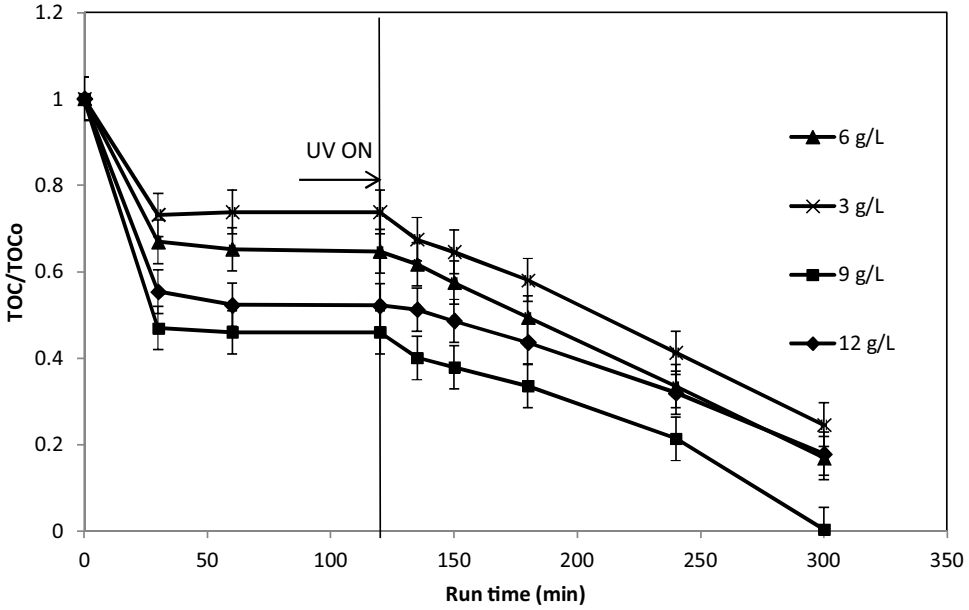

Fig. 12. Total Organic Carbon (TOC) removal over the Au-TiO_2(PD-HI) 15 min catayst, varying the dosage of the photocatalyst (g/L); patent blue V initial concentration: 7 mg/L.

dye concentration (12 mg/L), this system is able to predict the discoloration trend with a single value of kinetic constant. Thus the photocatalytic activity is not dependent by the increase of the intensity of the color meaning that the path length of photons inside the solution didn't decrease allowing to obtain in an effective way also the mineralization of the dye (Fig. 10).

3.2.3. *Patent blue V photodegradation on Au-TiO_2–Effect of the catalyst dosage*

The effect of the catalyst dosage over the effectiveness of the sample Au-TiO_2(PD-HI) 15min was evaluated in the range 3–12 g/L and the results of discoloration and TOC removal are presented in Figs. 11 and 12, respectively. After these experiments, it is possible to confirm that the best dosage of catalyst is 9 g/L, obtaining the highest discoloration and mineralization of PB. Photocatalytic efficiency increased as catalyst loading was increased up to 9 g/L. When the load of catalyst was increased from 9 to 12 g/L, the discoloration and the mineralization of the dye decreased. Possibly, the increase in the catalyst dosage over the optimum value resulted in a decreased light penetration through the solution because of the increased opacity of the aqueous suspension [22].

3.2.4. *Patent blue V photodegradation on Pt-TiO_2*

The effectiveness of the platinized samples in the dye photodegradation was also evaluated. Fig. 13 shows the evolution of the discoloration of the PB as a function of run time, obtained over Pt-TiO_2 photocatalysts in comparison with S-TiO_2. Also with these catalysts, in dark conditions a decrease of PB concentration was observed during the first 30 min of the test and it was almost unchanged up to 120 min. After the dark period, the solution was irradiated with UV light. During the irradiation time, it can be observed an increase of the dye degradation. The best discoloration

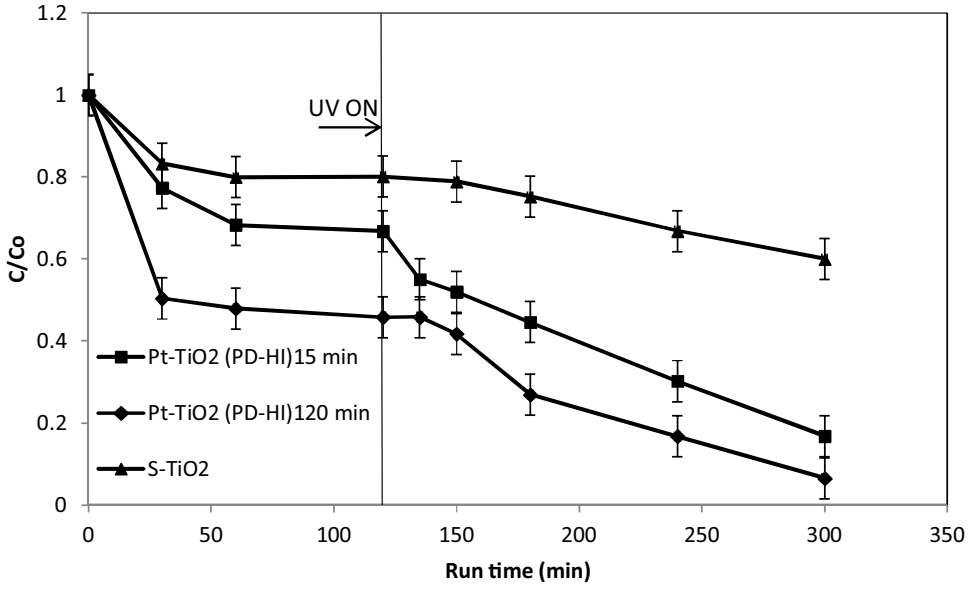

Fig. 13. Patent blue V discoloration over the Pt-TiO_2 photocatalyst prepared with 140 W/m^2 of light intensity and different deposition time (15 and 120 min); patent blue V initial concentration: 7 mg/L; catalyst dosage: 3 g/L.

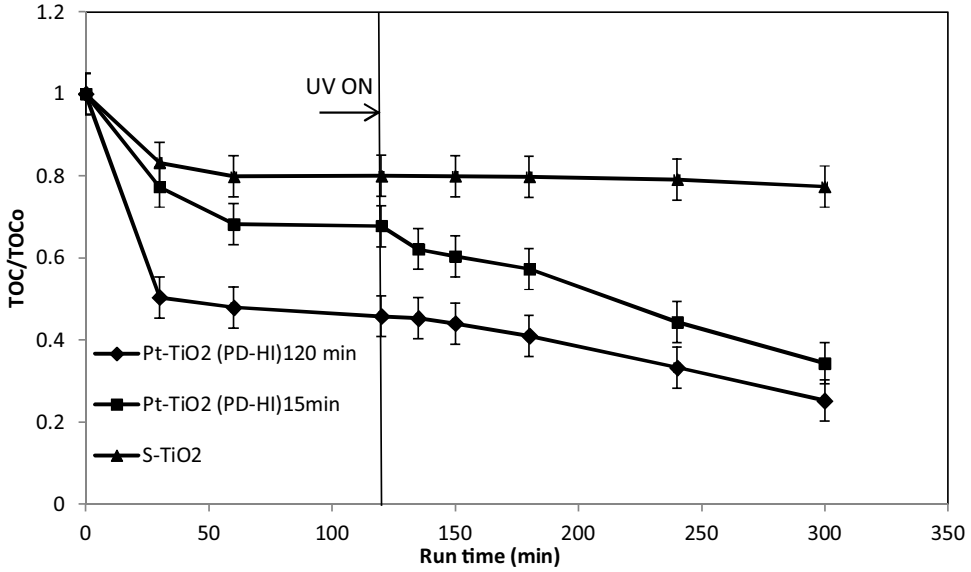

Fig. 14. Total Organic Carbon (TOC) removal over the Pt-TiO_2 photocatalyst prepared with 140 W/m^2 of light intensity and different deposition time (15 and 120 min); patent blue V initial concentration: 7 mg/L; catalyst dosage: 3 g/L.

(85%) and dye mineralization (44%) (Fig. 14) was obtained over the catalyst Pt-TiO_2 prepared by photochemical deposition method and using 120 min of deposition time in the synthesis. These results may be due to the higher Pt content of the photocatalyst prepared with the highest deposition time.

3.2.5. *Patent blue V photodegradation—effect of the kind of noble metal (Au or Pt)*

A comparison between the results obtained on the best Au-TiO_2 and Pt-TiO_2 photocatalysts is shown in Fig. 15. As it can be observed, the best performances are obtained with the Au-TiO_2 catalyst since the TOC removal and discoloration rate under UV irradiation are higher than that obtained for Pt-TiO_2 catalyst.

From the results reported in Table 1, it is possible to note that the catalyst Pt-TiO_2(PD-HI) 120min has Pt particle size comprised in the range 4–6 nm, while the catalyst Au-TiO_2(PD-HI) 15min has Au particle size in the range of 30–40 nm, so one would expect that the catalyst Pt-TiO_2(PD-HI) 120min presents a better photocatalytic activity. From the experimental results, instead, it is noted that the best photocatalytic efficiency is obtained with the catalyst in the presence of Au. In fact, the literature results reports that Au-TiO_2 shows higher catalytic activity than Pt [23]. Considering that the noble metals act as a mediator in the vectorial electron-transfer process, their Fermi energy levels are supposed to affect the interfacial charge transfer and thus the charge separation [24]. In general, the higher Fermi level of the noble metal leads to the better the photocatalytic activity [25]. In this context, it was found that, for Fermi level, the order of noble metals is of Au > Pt [26], explaining in this way, the better photocatalytic activity of Au-TiO_2 with respect to Pt-TiO_2 catalyst.

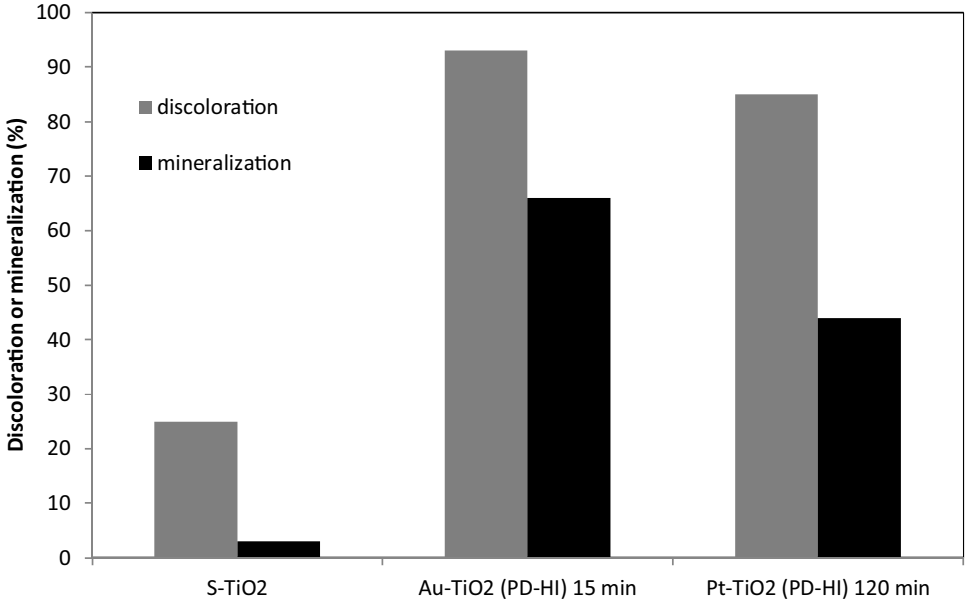

Fig. 15. Comparison of the patent blue V discoloration and mineralization over the S-TiO_2 and the most effective M-TiO_2 photocatalysts; Patent blue V initial concentration: 7 mg/L; catalyst dosage: 3 g/L.

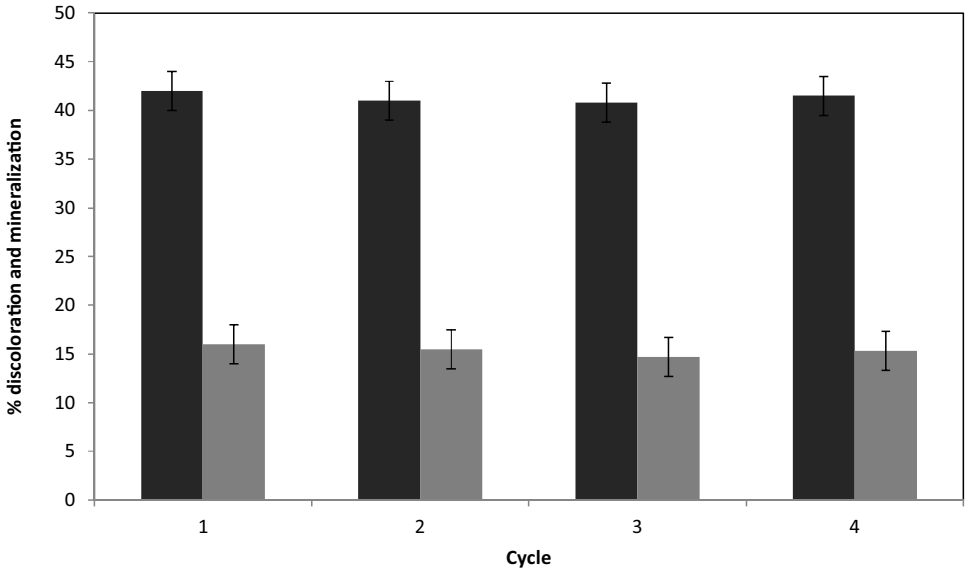

Fig. 16. Evaluation of Patent blue V discoloration and mineralization after 60 min of irradiation on Au-TiO_2(PD-HI) 15min catalyst for different cycles; patent blue V initial concentration: 4.7 mg/L; catalyst dosage: 3 g/L.

3.2.6. Recyclability of Au-TiO_2 photocatalyst

Recyclability is one of the most important factors in catalysis research [27,28]. To confirm the recyclability of Au-TiO_2(PD-HI) 15min sample, the photocatalytic degradation of PB was repeated up to four cycles (Fig. 16). The reduction of discoloration and mineralization percentage was as low as 1–2% in 60 min of irradiation time. So, these results evidenced the stability of the photocatalyst and the reproducibility of the process in the PB degradation.

4. Conclusion

In this work the photocatalytic removal of the PB dye with noble metals based photocatalysts has been addressed for the first time. In particular, it was tested the efficiency of photocatalysts based on gold or platinum deposited on the surface of sulfated titania, prepared by two different methods: chemical reduction (CR) and photochemical deposition (PD).

It was observed that the presence of Au or Pt on TiO_2 enhances the PB photodegradation and it was also found that metal distribution on TiO_2 and noble metal particle size are important factors influencing the dye degradation. There are significant differences in particles sizes and morphology between samples prepared by PD or by CR. In fact, for the Au-TiO_2 catalyst prepared by CR, the gold particles are more homogeneously distributed on TiO_2 surface than that observed in the samples prepared by PD. This causes a reduction in the value of the specific surface area for the sample prepared by CR.

The highest dye degradation was obtained over the Au-TiO_2 catalyst prepared by PD method, using high light intensity and 15 min of deposition time during the synthesis.

In this catalyst, the Au nanoparticles are heterogeneously distributed and present in lower number on TiO_2 surface, allows to the dye molecule to have a best contact with the TiO_2 surface.

For Pt-TiO_2 catalysts the best discoloration and dye mineralization were obtained over the catalyst prepared by photochemical deposition method and using 120 min of deposition time in the synthesis. These results may be due to the higher Pt content of the photocatalyst prepared with the highest deposition time. Comparing the performance of the different catalysts, it can be concluded that the presence of the noble metal on the TiO_2 surface enhances the removal efficiency of the dye and that in particular the catalyst with gold showed a better efficiency of removal of PB.

Acknowledgements

CITIUS (University of Seville) is acknowledged for XPS and XRF measurements. The authors wish to thank University of Salerno for funding the project "Sistemi catalitici per l'intensificazione di processo e per la riduzione dell'inquinamento ambientale" (Ex 60%, anno 2014).

References

[1] A. Duta, M. Visa, J. Photochem. Photobiol. A 306 (2015) 21–30.
[2] E. Kordouli, K. Bourikas, A. Lycourghiotis, C. Kordulis, Catal. Today 252 (2015) 128–135.
[3] J.J. Murcia, M.C. Hidalgo, J.A. Navio, J. Arana, J.M. Dona-Rodriguez, Appl. Catal B 150–151 (2014) 107–115.
[4] V. Vaiano, O. Sacco, G. Iervolino, D. Sannino, P. Ciambelli, R. Liguori, E. Bezzeccheri, A. Rubino, Appl. Catal B 176–177 (2015) 594–600.
[5] D. Sannino, V. Vaiano, P. Ciambelli, M.C. Hidalgo, J.J. Murcia, J.A. Navío, J. Adv. Oxid. Technol. 15 (2012) 284–293.
[6] J.J. Murcia, M.C. Hidalgo, J.A. Navío, V. Vaiano, D. Sannino, P. Ciambelli, Catal. Today 209 (2013) 164–169.
[7] A.V. Vorontsov, I.V. Stoyanova, D.V. Kozlov, V.I. Simagina, E.N. Savinov, J. Catal. 189 (2000) 360–369.
[8] W.Y. Teoh, L. Mädler, R. Amal, J. Catal. 251 (2007) 271–280.
[9] F. Denny, J. Scott, K. Chiang, W.Y. Teoh, R. Amal, J. Mol. Catal. A 263 (2007) 93–102.
[10] C. Hu, Y. Tang, J. Zheng, Z. Hao, H. Tang, P.K. Wong, Appl. Catal A 253 (2003) 389–396.
[11] M. Saquib, M. Abu Tariq, M. Faisal, M. Muneer, Desalination 219 (2008) 301–311.
[12] R.R. Dalbhanjan, N.S. Pande, B.S. Banerjee, S.P. Hinge, A.V. Mohod, P.R. Gogate, Desalin. Water Treat. (2015).
[13] C. Fernandez, M.S. Larrechi, M.P. Callao, Talanta 79 (2009) 1292–1297.
[14] G. Colon, M.C. Hidalgo, J.A. Navio, Appl. Catal B 45 (2003) 39–50.
[15] K. Okazaki, Y. Morikawa, S. Tanaka, K. Tanaka, M. Kohyama, Phys. Rev. B: Condens. Matter Mater. Phys. 69 (2004), 235404/235401–235404/235408.
[16] J. Kimling, M. Maier, B. Okenve, V. Kotaidis, H. Ballot, A. Plech, J. Phys. Chem. B 110 (2006) 15700–15707.
[17] B.K. Min, J.E. Heo, N.K. Youn, O.S. Joo, H. Lee, J.H. Kim, H.S. Kim, Catal. Commun. 10 (2009) 712–715.
[18] S. Link, M.A. El-Sayed, J. Phys. Chem. B 103 (1999) 4212–4217.
[19] M.C. Hidalgo, M. Maicu, J.A. Navio, G. Colon, J. Phys. Chem. C 113 (2009) 12840–12847.
[20] J.J. Murcia, M.C. Hidalgo, J.A. Navio, J. Arana, J.M. Dona-Rodriguez, Appl. Catal. B 179 (2015) 305–312.
[21] D. Sannino, V. Vaiano, O. Sacco, P. Ciambelli, J. Environ. Chem. Eng. 1 (2013) 56–60.
[22] V. Vaiano, G. Iervolino, G. Sarno, D. Sannino, L. Rizzo, J.J. Murcia Mesa, M.C. Hidalgo, J.A. Navío, Oil Gas Sci. Technol. 70 (2015) 891–902.
[23] M. Maicu, M.C. Hidalgo, G. Colón, J.A. Navío, J. Photochem. Photobiol. A 217 (2011) 275–283.
[24] J.B. Hudson, Surface Science: An Introduction, Wiley, 1998.
[25] S. Halas, T. Durakiewicz, J. Phys. Condens. Matter 10 (1998) 10815–10826.
[26] S. Shen, L. Guo, X. Chen, F. Ren, C.X. Kronawitter, S.S. Mao, Int. J. Green Nanotechnol Mater. Sci. Eng. 1 (2010) M94–M104.
[27] V. Vaiano, O. Sacco, D. Sannino, P. Ciambelli, Appl. Catal. B 170–171 (2015) 153–161.
[28] V. Vaiano, G. Iervolino, D. Sannino, L. Rizzo, G. Sarno, A. Farina, Appl. Catal. B 160-161 (2014) 247–253.